

# Measurement of the Spatial Cross-Correlation Function of Damped Lyman $\alpha$ Systems and Lyman Break Galaxies

Jeff Cooke<sup>1 2</sup> & Arthur M. Wolfe<sup>1</sup>

*Department of Physics and Center for Astrophysics and Space Sciences; University of California, San Diego, mc-0424, La Jolla, CA 92093-0424*

cooke@physics.ucsd.edu

awolfe@ucsd.edu

Eric Gawiser<sup>13</sup>

*Department of Astronomy; Yale University, P.O. Box 208101, New Haven, CT 06520-8101*

gawiser@astro.yale.edu

and

Jason X. Prochaska<sup>1</sup>

*UCO-Lick Observatory; University of California, Santa Cruz, Santa Cruz, CA 95064*

xavier@ucolick.edu

## ABSTRACT

We present the first spectroscopic measurement of the spatial cross-correlation function between damped Lyman  $\alpha$  systems (DLAs) and Lyman break galaxies (LBGs). We obtained deep  $u'$ BVRI images of nine QSO fields with 11 known  $z \sim 3$  DLAs and spectroscopically confirmed 211  $R < 25.5$  photometrically selected  $z > 2$  LBGs. We find strong evidence for an overdensity of LBGs near DLAs versus random, the results of which are similar to that of LBGs near other

---

<sup>1</sup>Visiting Astronomer, W. M. Keck Telescope. The Keck Observatory is a joint facility of the University of California, the California Institute of Technology, and NASA and was made possible by the generous financial support of the W. M. Keck Foundation.

<sup>2</sup>Center for Cosmology, University of California, Irvine, CA 92697; cooke@uci.edu

<sup>3</sup>NSF Astronomy & Astrophysics Postdoctoral Fellow

LBGs. A maximum likelihood cross-correlation analysis found the best fit correlation length value of  $r_0 = 2.9_{-1.5}^{+1.4} h^{-1} \text{Mpc}$  using a fixed value of  $\gamma = 1.6$ . The implications of the DLA-LBG clustering amplitude on the average dark matter halo mass of DLAs are discussed.

*Subject headings:* galaxies: high redshift — quasars: absorption lines — galaxies: formation — galaxies: evolution

## 1. Introduction

Over the last two decades, quasar (QSO) absorption line systems have provided tremendous insight into the nature of proto-galaxies at high redshift. Of particular interest are the damped Lyman  $\alpha$  systems (DLAs) defined to have  $N(\text{HI}) \geq 2 \times 10^{20} \text{ atoms cm}^{-2}$  (Wolfe et al. 1986, 2005). Systems with such large column densities can provide self-shielding from the ambient ionizing radiation at high redshift and protect large reservoirs of neutral gas. Such systems are prime sites for star formation. Moderate and high-resolution databases (e.g. Prochaska et al. 2001, 2003) and numerous spectroscopic studies of DLAs have given us a detailed view of the chemical abundances and gas kinematics of proto-galaxies, yet, except for two confirmed  $z > 2$  detections of DLA emission (Møller et al. 2002, 2004), information regarding their mass, luminosity, and morphology has remained elusive.

One approach to measure the average mass of a galaxy population at high redshift is under the implicit assumption that galaxies are a result of the gravitational instabilities of primordial density fluctuations. CDM hierarchical models predict that the most massive galaxies at high redshift preferentially form clustered together near the density peaks of regions with an underlying mass overdensity, whereas low-mass galaxies form more uniformly throughout space (Kaiser 1984; Bardeen et al. 1986). The factor in which the underlying dark matter is enhanced in the regions where galaxies cluster as compared to that implied by the galaxies themselves is referred to as bias. In this context, the spatial distribution of a population of galaxies provides a means to infer their typical dark matter halo mass. This method has been used to infer the average mass of Lyman break galaxies (LBGs) at  $z \sim 3$  (e.g. Steidel et al. 1998; Adelberger et al. 1998) and agrees with the mass estimates from nebular line-width measurements (Pettini et al. 2001) and those implied by star formation model fits (Shapley et al. 2001).

It is difficult to measure the mass of DLAs by their spatial clustering because of the sparse distribution of bright QSO sightlines and since only approximately one quarter of all  $z > 3$  QSOs exhibit DLA absorption. However, the mass of DLAs can be inferred by

their cross-correlation with another known population (Gawiser et al. 2001). Since the LBG auto-correlation function and LBG galaxy bias at  $z \sim 3$  has been established (Adelberger et al. 2003; hereafter A03), it is natural to use these galaxies as tracers of the underlying mass distribution to cross-correlate with  $z \sim 3$  DLAs. With this in mind, A03 used the spectroscopic sample of Steidel et al. (2003) to test the spatial distribution of LBGs and DLAs. A count of the number of LBGs in three-dimensional cells centered on the four DLAs in their sample showed no significant overdensity. In contrast, Bouché & Lowenthal (2004) used photometric redshifts to measure the clustering of LBGs near two DLAs and one sub-DLA in wide-field images. From Monte Carlo simulations, they found a non-zero DLA-LBG clustering amplitude to greater than  $2\sigma$  and angular analysis on scales out to  $\sim 20h^{-1}\text{Mpc}$  estimated the DLA-LBG cross-correlation to be equal to, or greater than, the LBG auto-correlation. Both analyses had limited statistics and could neither confirm, nor rule out, a significant overdensity of LBGs near DLAs.

In this Letter, we highlight the results of a spectroscopic survey for LBGs associated with 11 DLAs at  $z \sim 3$ . We introduce strong evidence for an overdensity of LBGs near DLAs and present the first detection of the three-dimensional DLA-LBG cross-correlation function. A more complete discussion of the DLA-LBG cross-correlation analysis is presented in Cooke et al. (2005b) along with our independent measurement of the  $z \sim 3$  LBG auto-correlation function. In this Letter, we adopt  $\Omega_M = 0.3, \Omega_\Lambda = 0.7$  cosmology.

## 2. Observations

We acquired deep  $u'$ BVRI images from 2000 April through 2003 November of nine QSO fields with 11 known DLAs ( $2.78 < z < 3.32$ ) using the Carnegie Observatories Spectrograph and Multi-Object Imaging Camera (Kells et al. 1998) on the 200" Hale telescope at Palomar and the Low Resolution Imager and Spectrometer (LRIS; Oke et al. 1995) on the Keck I telescope. The data were reduced in a standard manner. We developed a  $u'$ BVRI photometric selection technique for LBGs at  $z \sim 3$  that proved comparable to previous techniques in both efficiency and resulting redshift distribution. Over the 465 arcmin<sup>2</sup> surveyed, we found 796  $R < 25.5$  objects that met our color criteria. Follow-up multi-object spectroscopy of 529 LBG candidates using LRIS yielded 339 redshifts. We identified 211 LBGs with  $z > 2$  and used these in the cross-correlation analysis. Details of data acquisition, reduction, and analysis can be found in Cooke et al. (2005a).

### 3. Clustering Analysis

#### 3.1. Evidence of an LBG overdensity near DLAs

As a coarse measure of the distribution of LBGs near DLAs, we divided our survey volume into cells with dimensions of the field area of LRIS at  $z \sim 3$  ( $\sim 7 \times 10h^{-1}\text{Mpc}$ ) and  $\Delta z = 0.025$  ( $\sim 17h^{-1}\text{Mpc}$ ). The choice in cell size follows that of Adelberger et al. (1998) and includes the majority of the objects associated with a central object having a galaxy bias less than or equal to the LBG bias at  $z \sim 3$ . The extended length in the redshift direction is intended to account for the  $\sim 1 - 2h^{-1}\text{Mpc}$  error in the systemic redshift measurement inherent to LBGs.

This simple counts-in-cells analysis found an average of 1.27 objects residing in cells centered on each of the 11 DLAs where an average of 0.85 objects should have been found randomly. Random values were determined for objects in identical cells at the redshifts of the DLAs pulled from normalized random catalogs that mimicked the constraints of the data and were corrected by the photometric selection function [see Cooke et al. (2005a,b)]. This observed overdensity can be compared to an average of 1.16 objects found in cells of identical size centered on LBGs in our survey having similar redshifts to the DLAs but located in other fields. Interestingly, two of the 14 objects associated with the DLAs are QSOs. Since QSOs are believed to form in massive dark matter halos that seed supermassive black holes, this suggests that the corresponding DLAs reside in overdense regions.

#### 3.2. DLA-LBG cross-correlation function

We measured the DLA-LBG cross-correlation function  $\xi_{DLA-LBG}$  using the usual approach of comparing galaxy pair separations in the data to galaxy pair separations in the random galaxy catalogs. We used the estimator of Landy & Szalay (1993) to measure the excess probability over random of finding an LBG at a distance  $r$  from a DLA

$$\xi_{DLA-LBG}(r) = \frac{D_{DLA}D_{LBG} - D_{DLA}R_{LBG} - R_{DLA}D_{LBG} + R_{DLA}R_{LBG}}{R_{DLA}R_{LBG}} \quad (1)$$

where  $D_{DLA}D_{LBG}$  is the catalog of data-data pair separations,  $D_{DLA}R_{LBG}$  and  $R_{DLA}D_{LBG}$  are the data-random and random-data pair separation cross-reference catalogs, and  $R_{DLA}R_{LBG}$  is the catalog of random-random pair separations. This estimator is well-suited for small galaxy samples and has a nearly Poisson variance. The random catalogs were constructed to be many times larger than the data catalog to reduce shot noise and were then normalized to the data. The mean LBG density was determined from the data in all 11 fields. We

determined  $\xi(r)$  by counting the number of pairs in each catalog over a series of log or linear intervals (i.e. bins). In addition, we made the assumption that  $\xi(r)$  follows a power law of the form

$$\xi(r) = \left(\frac{r}{r_0}\right)^{-\gamma}. \quad (2)$$

### 3.3. Conventional binning

We initially measured the cross-correlation function by duplicating the cylindrical binning technique described in A03, Appendix C. This technique was adopted to help minimize the effect that LBG redshift uncertainties have on the clustering signal as compared to traditional radial bins. In addition, this approach permitted a direct comparison of our results to the published LBG auto-correlation values of A03 using the available online dataset<sup>1</sup> of Steidel et al. (2003) since both surveys were executed in a similar manner and used the same instruments and configurations.

In this treatment, the expected projected angular overdensity is defined to be

$$\omega_p(r_\theta) \equiv \frac{r_0^\gamma r_\theta^{1-\gamma}}{2r_z} B\left(\frac{1}{2}, \frac{\gamma-1}{2}\right) I_x\left(\frac{1}{2}, \frac{\gamma-1}{2}\right) \quad (3)$$

where  $r_z$  is the greater of  $1000 \text{ km sec}^{-1}(1+z)/H(z)$  and  $7r_\theta$ , and  $B$  and  $I_x$  are the beta and incomplete beta functions with  $x \equiv r_z^2(r_z^2 + r_\theta^2)^{-1}$  (Press et al. 1992). Applying this method to the DLA-LBG cross-correlation, we found best fit parameter values and 1 sigma uncertainties of  $r_0 = 3.3 \pm 1.3h^{-1}\text{Mpc}$ ,  $\gamma = 1.7 \pm 0.4$ . Figure 1 presents and compares these results with the LBG auto-correlation results of A03 and is plotted in a consistent manner where  $r_{max} = r_z$  as described above. The errors on the cross-correlation values shown in the figure are those determined using the formulation in Landy & Szalay (1993) and the reported errors on the functional fit were determined by duplicating the Monte Carlo error analysis as described in A03. The latter error analysis may underestimate the true error by a factor of  $\sim 1 - 2$  (Adelberger et al. 2005).

Although the uncertainties are large, it is immediately apparent from Figure 1 that the form and central values of the two correlation functions are similar. In addition, we computed a cross-correlation length of  $r_0 = 3.5 \pm 1.0h^{-1}\text{Mpc}$  for a fixed value of  $\gamma = 1.6$ , equivalent to the value reported in A03 and Adelberger et al. (2005) for the LBG auto-correlation. Our decision to center the DLAs in the observed fields prevented an estimation

---

<sup>1</sup><http://vizier.cfa.harvard.edu/viz-bin/VizieR?-source=J/ApJ/592/728/>

of the DLA-LBG cross-correlation effectively beyond  $\sim 4h^{-1}\text{Mpc}$  using the above method. However, our cross-correlation values are consistent with the constraints placed on the DLA-LBG cross-correlation by Bouché & Lowenthal (2004) using a comparable analysis over a range of  $\sim 5 - 15h^{-1}\text{Mpc}$ .

### 3.4. Maximum likelihood

As an independent method of analysis, and to make the most of our dataset, we determined the maximum likelihood of a power law fit (equation 2) to the observed data (e.g. Croft et al. 1997; Mullis et al. 2004). We divided the radial separations into a large number of finely spaced regular intervals that coincided with either 1 or 0 LBGs. Poisson statistics hold in the regime of large interval number and small probability per interval. We used this to form the likelihood function

$$\mathcal{L} = \prod_i^N \frac{e^{-\mu_i} \mu_i^{\nu_i}}{\nu_i!} \prod_{j \neq i}^N \frac{e^{-\mu_j} \mu_j^{\nu_j}}{\nu_j!} \quad (4)$$

where  $\mu_i$  is the expected number of pairs in the  $i$ th interval,  $\nu_i$  is the observed number of pairs for that same interval, and the index  $j$  runs over the elements where there are no pairs. The expected number of pairs was determined by solving equation 1 for  $D_{DLA}D_{LBG}$  over a reasonable range of  $r_0$  and  $\gamma$ . We then maximized the expression  $S = -2 \ln \mathcal{L}$ . Confidence levels were defined as  $\Delta S = S(r_{0,best}, \gamma_{best}) - S(r_0, \gamma)$  with the assumption that  $S$  has a  $\chi^2$  distribution. We found the best fit values and 68% confidence levels for the cross-correlation using this method to be  $r_0 = 2.8_{-2.0}^{+1.4}h^{-1}\text{Mpc}$ ,  $\gamma = 2.1_{-1.4}^{+1.3}$  and a best fit value of  $r_0 = 2.9_{-1.5}^{+1.4}h^{-1}\text{Mpc}$  for a fixed  $\gamma = 1.6$ . Figure 2 displays these results.

Cooke et al. (2005b) describe the above analyses in more detail, present several tests to address the shortcomings of each method, and make efforts to quantify the physical effects that the multi-object slitmasks have on the clustering signal. A short summary of best fit values and  $1\sigma$  uncertainties described here and from that work is listed in Table 1. It can be seen that all independent methods, and tests thereof, result in consistent central values within their uncertainties.

## 4. Discussion

The LBG bias at  $z \sim 3$ , derived from the LBG auto-correlation of the  $R < 25.5$  spectroscopic sample, indicates an average LBG dark matter halo mass of  $\sim 10^{12}M_{\odot}$  (e.g. Steidel

et al. 1998; Adelberger et al. 1998). The 11 DLAs presented here comprise an unbiased representation of a random cross-section weighted sample. The similarity between the LBG auto-correlation and the DLA-LBG cross-correlation implies that the bias factors of the two populations are comparable and that DLAs, on average, may form in similarly massive potential wells. We consider the implications from the best fit central value  $r_0 \sim 2.9$  using the maximum likelihood method with fixed  $\gamma = 1.6$ . This measurement corresponds to a DLA galaxy bias of  $b_{DLA} \sim 2.4$  and represents an average DLA halo mass of  $\langle M_{DLA} \rangle \sim 10^{11.2} M_\odot$ . This value is higher than what is predicted for DLAs by simple models (e.g. Mo et al. 1998) but is in very good agreement with numerical models of varying resolution that invoke strong galactic-scale winds (Nagamine et al. 2005) and thermal feedback (Maller et al. 2001; Bouché et al. 2005). In these models, galactic outflows purge low-mass halos of gas capable of generating damped Lyman  $\alpha$  absorption lines and result in a higher mean mass. It must be noted that because CDM predicts a steeply rising mass function, it is expected that the median DLA halo mass is lower than the mean mass implied here.

The observed similarity in the spatial distributions of DLAs and LBGs also helps support previous ideas that the two populations may be connected (Schaye 2001; Møller et al. 2002). Recent analysis of the *Hubble Ultra Deep Field* (Chen & Wolfe 2005) shows little evidence for *in situ* star formation throughout the DLA neutral gas. However, calculations using the CII\* absorption feature to trace the cooling rates in DLAs (Wolfe et al. 2003) require local sources of radiation to heat DLAs. A plausible scenario is that LBGs are embedded in the same systems that contain DLAs. This model is reinforced by the near equality between DLA cooling rates and LBG heating rates. Furthermore, the lack of detected DLA emission out to reasonable impact parameters from background QSOs and the above implied average halo mass are consistent with DLAs sampling the bulk of the LBG population with typical impact parameters of  $< 1''$  and median luminosities of  $R > 27$ .

Although the uncertainties in this initial measure of the three-dimensional DLA-LBG cross-correlation function are large, there remains strong evidence for an overdensity of LBGs near DLAs. The similarity in the central values between the DLA-LBG cross-correlation and the LBG auto-correlation underscore a need for additional observations to improve the statistical significance of these results and to provide a step toward a complete picture of galaxy formation and evolution.

We would like to thank K. L. Adelberger and C. Mullis for helpful and informative discussions. This work was partially supported by the National Science Foundation grant AST-0307824 and the NSF Astronomy & Astrophysics Postdoctoral Fellowship (AAPF) grant AST-0201667 awarded to Eric Gawiser.

## REFERENCES

- Adelberger, K. L., Steidel, C. C., Giavalisco, M., Dickinson, M., Pettini, M., & Kellogg, M. 1998, *ApJ*, 505, 18
- Adelberger, K. L., Steidel, C. C., Shapley, A. E., & Pettini, M. 2003, *ApJ*, 584, 45
- Adelberger, K. L., Steidel, C. C., Pettini, M., Shapley, A. E., Reddy, N. A., & Erb, D. K. 2005, *ApJ*, 619, 697
- Bardeen, J.M., Bond, J.M., Kaiser, N., & Szalay, A.S. 1986, *ApJ*, 304, 15
- Bouché N. & Lowenthal, J. D. 2003, *ApJ*, 609, 513
- Bouché N., Gardner, J. P., Katz, N., Weinberg, D. H., Davé, R., & Lowenthal, J. D. 2005, *ApJ*, 628, 89
- Chen, H. W. & Wolfe, A. M. 2005, in preparation
- Cooke, J., Wolfe, A. M., Prochaska, J. X., & Gawiser, E. 2005 *ApJ*, 621, 596
- Cooke, J., Wolfe, A. M., Gawiser, E., Prochaska, J. X., 2005, in preparation
- Croft, R. A. C., Dalton, G. B., Efstathiou, G., Sutherland, W. J., & Maddox, S. J. 1997, *MNRAS*, 291, 305
- Gawiser, E., Wolfe, A. M., Prochaska, J. X., Lanzetta, K. M., Yahata, N., & Quirrenbach, A. 2001, *ApJ*, 562, 628
- Kaiser, N. 1984, *ApJ*, 284, 9
- Kauffmann, G. 1996, *MNRAS*, 281, 475
- Kells, W., Dressler, A., Sivaramakrishnan, A., Carr, D., Koch, E., Epps, H., Hilyard, D., & Pardeilhan, G. 1998, *PASP*, 110, 1487
- Landy, S. D. & Szalay, A. S. 1993, *ApJ*, 412, 64
- Maller, A. H., Prochaska, J. X., Somerville, R. S., & Primack, J. R. 2001, *MNRAS*, 326, 1475
- Mo, H. J., Mao, S., & White, S. D. M. 1998, *MNRAS*, 295, 319
- Møller, P., Warren, S. J., Fall, S. M., Fynbo, J. U., & Jakobsen, P. 2002, *ApJ*, 574, 51



- Møller, P., Fynbo, J. P. U., & Fall, S. 2004, *A&A*, 422, 33
- Mullis, C. R., Henry, J. P., Gioia, I. M., Böhringer, H., Briel, U. G., Voges, W., & Huchra, J. P. 2004, *ApJ*, 617, 192
- Nagamine, K., Wolfe, A. M., Springel, V., & Hernquist, L. 2005, *MNRAS*, in prep., astro-ph/0510729
- Oke, J. B. et al. 1995, *PASP*, 107, 375
- Pettini, M., Shapley, A. E., Steidel, C. C., Cuby, J-G., Dickinson, M., Moorwood, A. F. M., Adelberger, K. L., & Giavalisco, M. 2001, *ApJ*, 554, 981
- Press, W. H., Teukolsky, S. A., Vetterling, W. T., & Flannery, B. P. 1992 *Numerical Recipes in C. The Art of Scientific Computing*, Cambridge: University Press
- Prochaska, J. X., Wolfe, A. M., Tytler, D., Burles, S., Cooke, J., Gawiser, E., Kirkman, D., O’Meara, J. M., & Storrie-Lombardi, L. 2001, *ApJS*, 137, 21
- Prochaska, J. X., Gawiser, E., Wolfe, A. M., Cooke, J., & Gelino, D. 2003, *ApJS*, 147, 227
- Schaye, Joop 2001, *ApJ*, 559, 1
- Steidel, C. C., Adelberger, K. L., Giavalisco, M., Dickinson, M., Pettini, M., & Kellogg, M. 1998, *ApJ*, 492, 428
- Shapley, A. E., Steidel, C. C., Adelberger, K. L., Dickinson, M., Giavalisco, M., & Pettini, M. 2001, *ApJ*, 562, 95
- Steidel, C. C., Adelberger, K. L., Shapley, A. E., Pettini, M., Dickinson, M., & Giavalisco, M. 2003, *ApJ*, 592, 728
- Wolfe, A. M., Turnshek, D. A., Smith, H. E., & Cohen, R. D. 1986, *ApJS*, 61, 249
- Wolfe, A. M., Lanzetta, K. M., Foltz, C. B., & Chaffee, F. H. 1995, *ApJ*, 454, 698
- Wolfe, A. M., Prochaska, J. X., & Gawiser, E., 2003, *ApJ*, 593, 215
- Wolfe, A. M., Gawiser, E. & Prochaska, J.X. 2005, *ARA&A* 43, 861

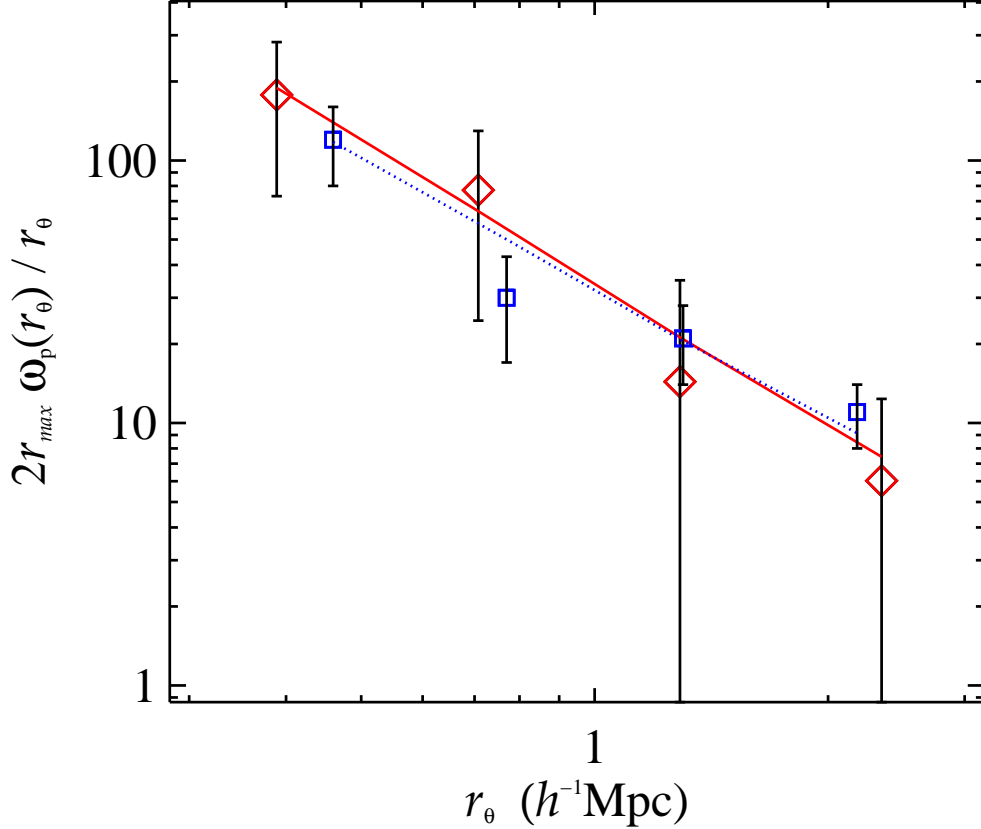


Fig. 1.— Measurement of the DLA-LBG cross-correlation following the binning method of Adelberger et al. (2003) and plotted in a consistent manner. The cross-correlation values are indicated by red diamonds and we find a best fit of  $r_0 = 3.3 \pm 1.3 h^{-1}\text{Mpc}$ ,  $\gamma = 1.7 \pm 0.4$  indicated by the solid red line. The errors shown are near Poisson and the reported errors are where 68% of the best fit values lie from a Monte Carlo analysis of the functional fit. For a fixed value of  $\gamma = 1.6$ , we find a best fit correlation length of  $r_0 = 3.5 \pm 1.0 h^{-1}\text{Mpc}$ . The LBG auto-correlation (blue squares) of Adelberger et al. (2003) are overlaid over a similar scale with the published fit of  $r_0 = 3.96 \pm 0.29 h^{-1}\text{Mpc}$ ,  $\gamma = 1.55 \pm 0.15$  (blue dotted line). The DLA-LBG cross-correlation values are consistent with the angular wide-field analysis of Bouché & Lowenthal (2004) significant on scales of  $\sim 5 - 10 h^{-1}\text{Mpc}$ .

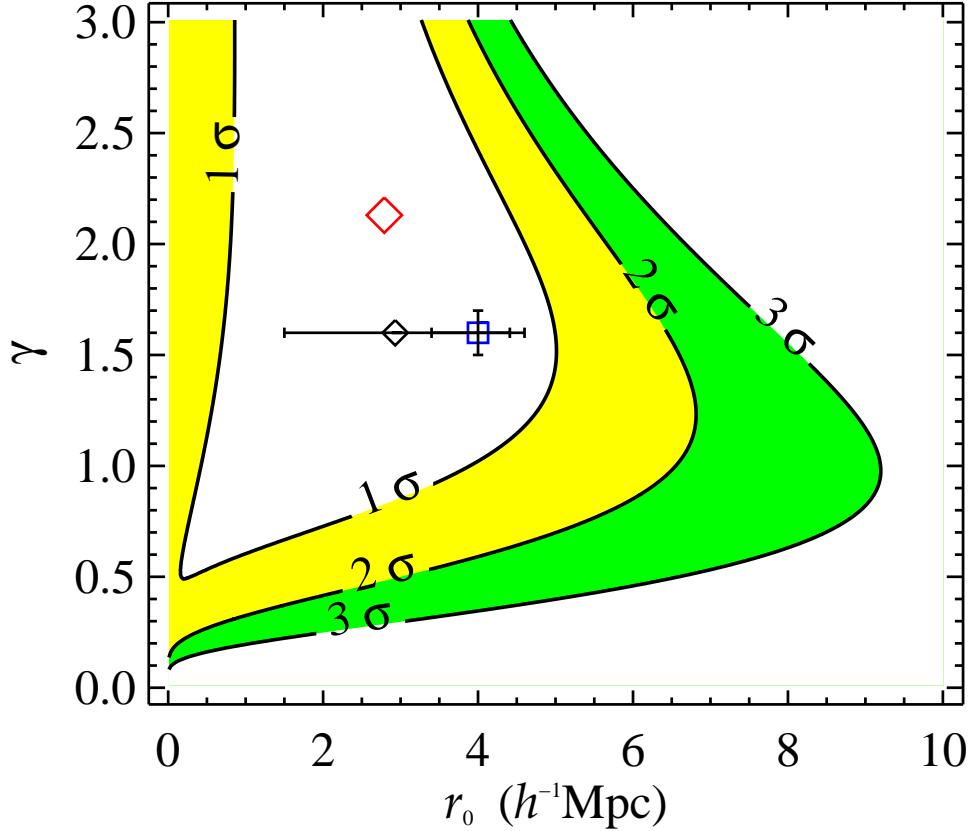


Fig. 2.— Two parameter probability contours for the DLA-LBG cross-correlation using the maximum likelihood method. The best fit values of  $r_0 = 2.8^{+1.4}_{-2.0} h^{-1} \text{Mpc}$ ,  $\gamma = 2.1^{+1.3}_{-1.4}$  are indicated by the large red diamond. The best fit value of  $r_0 = 2.9^{+1.4}_{-1.5} h^{-1} \text{Mpc}$  for a fixed value of  $\gamma = 1.6$  (small black diamond) is shown with the associated  $1\sigma$  uncertainty on  $r_0$ . For comparison, the blue square and error bars indicate the LBG auto-correlation best fit values and  $1\sigma$  uncertainties of  $4.0 \pm 0.6 h^{-1} \text{Mpc}$ ,  $\gamma = 1.6 \pm 0.1$  from Adelberger et al. (2005). Here, the angular positions of the galaxies in the random catalogs were made to be identical to the data to minimize possible artificial clustering effects caused by the physical constraints of the slitmasks.

Table 1. DLA-LBG Cross-Correlation Parameter Summary

Method	$r_0$	$\gamma$
Conventional binning <sup>a b</sup>	$3.32 \pm 1.3$	$1.74 \pm 0.4$
Maximum likelihood <sup>b c</sup>	$2.81^{+1.4}_{-2.0}$	$2.11^{+1.3}_{-1.4}$
Cumulative $\chi^2$ test <sup>b c d</sup>	$3.84^{+4.2}_{-3.8}$	$2.06^{+2.0}_{-1.3}$
Conventional binning <sup>a d e</sup>	$3.21 \pm 1.0$	$2.03 \pm 0.2$
Maximum likelihood <sup>c d e</sup>	$3.20^{+2.2}_{-2.9}$	$1.62^{+1.4}_{-1.0}$
Cumulative $\chi^2$ test <sup>c d e</sup>	$3.91^{+4.4}_{-3.9}$	$2.11^{+2.7}_{-1.3}$

<sup>a</sup>Galaxy separations binned using the cylindrical approach described in Adelberger et al. (2003), Appendix C

<sup>b</sup>Angular positions of galaxies in the random catalogs are identical to the angular positions of the data (to minimize possible artificial clustering effects caused by the slitmasks)

<sup>c</sup>Galaxy separations binned radially

<sup>d</sup>Described in Cooke et al. (2005b)

<sup>e</sup>Angular positions of galaxies in the random catalogs are random